14th International Conference on Information Fusion
Chicago, Illinois, USA, July 5-8, 2011

# Forecasting Probability of Target Presence for Ping Control in Multistatic Sonar Networks using Detection and Tracking Models

**Cherry Y. Wakayama**
Code 56560
SPAWAR Systems Center Pacific
San Diego, CA, U.S.A.
cherry.wakayama@navy.mil

**Doug J. Grimmett**
Code 56560
SPAWAR Systems Center Pacific
San Diego, CA, U.S.A.
doug.grimmett@navy.mil

**Zelda B. Zabinsky**
Industrial & Systems Engineering
University of Washington
Seattle, WA, U.S.A.
zelda@u.washington.edu

***Abstract*—This paper describes the forecasting of probability of target presence in a search area (also referred to as the PT map) considering both detection and non-detection conditions. Tracking results are also incorporated to obtain a more accurate PT map under the detection condition. The probability of target presence is a suitable metric for real-time ping control for a submarine search mission, whose objective is to quickly identify and localize as many targets as possible within the search area. Existing formulations of the probability of target presence metric for ping control include an open-loop approach in which measurements are ignored or a semi-adaptive approach in which measurements are considered but without the true/false target investigation. Since false contacts are inevitable in practical applications and the true/false target investigation of the contacts is not immediate, tracking results must be considered in the PT map generation to obtain an accurate assessment of the present and projected operational pictures. We develop an approach to obtain the current and forecasted PT maps by incorporating a measurement model, a sonar performance model, Bayes theorem and a centralized Kalman-Filter based tracker. The PT map is composed of two portions: the portion which contains detected target probability and the portion which contains missed target probability. Each portion of the PT map is updated and propagated separately. The forecasted PT map at the next ping time is obtained by combining the two propagated PT maps. It will be demonstrated by simulations that the combined forecasted PT map represents an accurate multistatic operational picture and can be used with a sonar performance model to obtain a field metric for ping control optimization for the area search mission.**

**Keywords: Ping control, sensor management, multistatic tracking.**

## I. Introduction

Multistatic active sonar networks provide an Anti-Submarine Warfare (ASW) capability against small, quiet, threat submarines in the harsh clutter-saturated littoral and deeper ocean environments through the expanded geometric diversity of a distributed field of sources and receivers. However, such networks cannot automatically exploit their full potential without intelligent management and control methods for the sources and receivers because of the variability in acoustic environmental conditions, sensor performance and threat target behavior [1]. In general, control methods and tactical decision aides may be applied to address the sensor placement, signal and information processing or sonar ping control problems. In addition, the control methods and metrics for dealing with threat submarines may be mission dependent in order to effectively optimize the sensor network performance for the given mission objective(s). This paper is concerned with the sensor ping control method for the area search mission type, whose objective is to *quickly* identify and localize as many threat targets as possible. In this case, the probability of target presence is an effective metric, and the adaptive control approach, in which the evaluation and optimization of the metric make use of all the information obtained during the operation to enhance real-time target Detection, Classification, and Localization (DCL) performance, is appropriate. In other cases, the mission may be to ensure that some selected area is free of threat targets. As discussed in [2], the ASW Residual Risk metric is an effective metric for the area clearance mission type and the sensor control approach may be optimized prior to the operation.

Approaches to evaluating the probability of target presence metric for ping control solutions for the area search mission are presented in [3] and [4]. The formulation presented in [3] ignore the measurements and assumes that no detection has been confirmed. The probability of target presence in each xy grid cell within the search area (also referred to as the PT map) is updated in a Bayesian manner under the non-detection hypothesis. In [4], the measurements are considered in the formulation and the PT map is updated in a Bayesian manner under the detection hypothesis if there is a measurement in the xy grid cell or under the non-detection hypothesis otherwise. In both formulations, the forecasted PT map is obtained by propagating the posterior probability using a diffusion process model. In the presence of false contacts, which is inevitable in practical applications, one must also account for the track consistency in order to discriminate the target-originated contacts against the contacts that are likely to be false alarms for obtaining accurate multistatic operational pictures. The true/false target investigation is not considered in the existing formulations.

# Report Documentation Page

*Form Approved*
*OMB No. 0704-0188*



| 1. REPORT DATE | 2. REPORT TYPE | 3. DATES COVERED |
|---|---|---|
| **JUL 2011** | | **00-00-2011 to 00-00-2011** |

| 4. TITLE AND SUBTITLE | 5a. CONTRACT NUMBER |
|---|---|
| **Forecasting Probability of Target Presence for Ping Control in Multistatic Sonar Networks using Detection and Tracking Models** | 5b. GRANT NUMBER |
| | 5c. PROGRAM ELEMENT NUMBER |
| 6. AUTHOR(S) | 5d. PROJECT NUMBER |
| | 5e. TASK NUMBER |
| | 5f. WORK UNIT NUMBER |
| 7. PERFORMING ORGANIZATION NAME(S) AND ADDRESS(ES) **SPAWAR Systems Center Pacific,Code 56560,San Diego,CA** | 8. PERFORMING ORGANIZATION REPORT NUMBER |
| 9. SPONSORING/MONITORING AGENCY NAME(S) AND ADDRESS(ES) | 10. SPONSOR/MONITOR'S ACRONYM(S) |
| | 11. SPONSOR/MONITOR'S REPORT NUMBER(S) |

12. DISTRIBUTION/AVAILABILITY STATEMENT

**Approved for public release; distribution unlimited**

13. SUPPLEMENTARY NOTES

**Presented at the 14th International Conference on Information Fusion held in Chicago, IL on 5-8 July 2011. Sponsored in part by Office of Naval Research and U.S. Army Research Laboratory.**

14. ABSTRACT

**This paper describes the forecasting of probability of target presence in a search area (also referred to as the PT map) considering both detection and non-detection conditions. Tracking results are also incorporated to obtain a more accurate PT map under the detection condition. The probability of target presence is a suitable metric for real-time ping control for a submarine search mission, whose objective is to quickly identify and localize as many targets as possible within the search area. Existing formulations of the probability of target presence metric for ping control include an open-loop approach in which measurements are ignored or a semi-adaptive approach in which measurements are considered but without the true/false target investigation. Since false contacts are inevitable in practical applications and the true/false target investigation of the contacts is not immediate, tracking results must be considered in the PT map generation to obtain an accurate assessment of the present and projected operational pictures. We develop an approach to obtain the current and forecasted PT maps by incorporating a measurement model, a sonar performance model, Bayes theorem and a centralized Kalman-Filter based tracker. The PT map is composed of two portions: the portion which contains detected target probability and the portion which contains missed target probability. Each portion of the PT map is updated and propagated separately. The forecasted PT map at the next ping time is obtained by combining the two propagated PT maps. It will be demonstrated by simulations that the combined forecasted PT map represents an accurate multistatic operational picture and can be used with a sonar performance model to obtain a field metric for ping control optimization for the area search mission.**

15. SUBJECT TERMS

| 16. SECURITY CLASSIFICATION OF: | | | 17. LIMITATION OF ABSTRACT | 18. NUMBER OF PAGES | 19a. NAME OF RESPONSIBLE PERSON |
|---|---|---|---|---|---|
| a. REPORT<br>**unclassified** | b. ABSTRACT<br>**unclassified** | c. THIS PAGE<br>**unclassified** | **Same as Report (SAR)** | **8** | |

**Standard Form 298 (Rev. 8-98)**
Prescribed by ANSI Std Z39-18

We develop an approach to construct the PT maps which considers the measurements (sonar contacts) as well as the true/false target investigation of the contacts (via tracking) and evaluates true and false target probabilities, missed target probabilities and no target probabilities by incorporating a sonar performance model, a measurement model, Bayes theorem, and a multistatic target tracker (MTT). We assume that an xy-grid-based probability of detection map for each source-receiver-waveform combination is provided by a sonar performance model. Our objective is to obtain xy-grid-based PT maps at the current and next ping times from the measurements and the tracker outputs. In addition to the PT maps, it is also required to obtain the multiple-target state estimates. While performing the area search mission, it is desired to track not only the possible target-originated contacts but also the area that has been not been searched. The complete PT maps should contain information resulting from the presence and absence of contacts in the area that has been searched.

A portion of the probability of target presence in each grid cell due to the possible target-originated contacts is obtained from the multiple-target state estimates of the tracker. The missed detection probability in the area that has been searched is obtained by incorporating a sonar performance model, a measurement model and Bayes theorem. The tracker in this work is a conventional centralized Kalman-Filter (KF) based tracker which performs explicit data associations between measurements and targets to update the multiple-target state estimates [5]. This tracker does not assume any *a priori* distribution of targets and does not account for the missed targets until tentative tracks have been initiated.

Alternatively, the PT maps may also be generated from the implementations of Probability Hypothesis Density (PHD) filter [6] and [7]. The PHD filter operates on the single-target state space and avoids the explicit data association between measurements and targets. It is a recursion that propagates the first-order statistical moment, or intensity, of the random finite set of states according to given model parameters that define target survival probability and the shapes of target birth and spawning intensities [7] and [8]. In order to obtain the multiple-target state estimates, one must then perform peak extraction from the posterior intensity. In this paper, we assume the use of a conventional KF based tracker and develop a formulation for the PT map.

This paper proceeds as follows. In Section II, we describe the formulation of the probability of target presence forecaster. We present simulation results to demonstrate the performance of the forecaster in Section III. Conclusions and future work are provided in Section IV.

## II. Formulation of Probability of Target Presence Forecaster

The objective of the forecaster is to obtain accurate operational pictures of the multistatic network for real-time ping control by evaluating true and false target probabilities, missed target probabilities as well as no target probabilities. This is achieved by updating PT maps after each ping using Bayes theorem under the detection and non-detection hypotheses separately. The tracking (true/false target investigation) results are incorporated to further refine the PT map under the detection hypothesis. We refer to the two PT maps generated under the detection and non-detection hypotheses as the positive PT map and the negative PT map, respectively, for the ease of discussion. The positive PT map describes the detected target probability and the negative PT map describes the missed target probability. The mathematical description of the forecaster is given in the following.

We define a search region on a xy coordinate space. We discretize the search region into a grid $G = [g_1, g_2, \cdots, g_{N_g}]^T$ where $g_i = \{(x,y), x \in [x_i - \delta/2, x_i + \delta/2), y \in [y_i - \delta/2, y_i + \delta/2)\}$, $N_g$ is the total number of grid cells, $(x_i, y_i)$ represents the center coordinates of cell $i$, and $\delta$ is the width of each cell. The state vector at time $t_k$ on $G$ is represented by $\mathcal{T}(k) = [T_1(k), T_2(k), \cdots, T_{N_g}(k)]^T$, where $T_i(k)$ is a binary random variable: $T_i(k) = 1$ represents the event that at least one target is in cell $i$ at time $t_k$, and $T_i(k) = 0$ represents the event that no target is in cell $i$. The PT map at time $t_k$ is defined as $[\mathrm{P}(T_1(k) = 1), \mathrm{P}(T_2(k) = 1), \cdots, \mathrm{P}(T_{N_g}(k) = 1)]^T$. Note that the summation of the probabilities on the PT map represents the expected number of targets in the search region.

We denote the set of measurement contacts at time $t_k$ by $\check{\mathcal{Z}}(k) = \{\mathcal{Z}^1(k), \mathcal{Z}^2(k), \cdots, \mathcal{Z}^{n_R}(k)\}$, where $n_R$ is the number of receivers. The measurement set at receiver $j$ at time $t_k$ is represented by $\mathcal{Z}^j(k) = \{Z_1^j(k), Z_2^j(k), \cdots, Z_{n_j}^j(k)\}$, where $n_j$ is the total number of contacts at receiver $j$. We model each measurement variable $Z_q^j$ as a Gaussian distribution with a mean vector of $[x_q^j, y_q^j]^T$ and a covariance matrix of $R_q^j$ for $q = 1, 2, \cdots, n_j$ and $j = 1, 2, \cdots, n_R$. The mean vector and covariance matrix are derived from the time-of-arrival and bearing measurements of contact $q$ at receiver $j$ and their associated measurement errors as described in [9].

We define an observation vector at time $t_k$ on $G$, which is denoted by $\mathcal{Y}(k) = [Y_1(k), Y_2(k), \cdots, Y_{N_g}(k)]^T$, where $Y_i(k)$ is a binary random variable: $Y_i(k) = 1$ represents the event that measurement observation occurs in cell $i$, and $Y_i(k) = 0$ represents the event that no measurement observation is in cell $i$. We refer to the event $Y_i = 1$ as the detection hypothesis and $Y_i = 0$ as the non-detection hypothesis.

### A. Bayes Update

For the ping generated at time $t_k$, we receive $n_j$ contacts at receiver $j$. We are going to suppress $k$ for ease of notation. The probability that the measurement data $Z_q^j$ occurs in cell $i$ is given by:

$$\mathrm{P}((Y_i)_q^j = 1 | Z_q^j) = \int_{(x,y) \in g_i} \mathcal{N}([x_q^j, y_q^j]^T, R_q^j) dx dy, \quad (1)$$

where $\mathcal{N}(m, \Sigma)$ denotes a Gaussian density with mean $m$ and covariance $\Sigma$, and $(Y_i)_q^j = 1$ represents the detection hypothesis with respect to measurement $q$ of receiver $j$. Aggregating the probability information across all contacts at receiver $j$, the probability that there is a measurement

observation in cell $i$ is obtained as:

$$\mathrm{P}(Y_i^j = 1|\mathcal{Z}^j) = \min\left(1, \sum_{q=1}^{n_j} \mathrm{P}((Y_i)_q^j = 1|Z_q^j)\right). \quad (2)$$

The probability that there is no measurement observation in cell $i$ after considering the measurement data $\mathcal{Z}^j$ at receiver $j$ is given by:

$$\mathrm{P}(Y_i^j = 0|\mathcal{Z}^j) = 1 - \mathrm{P}(Y_i = 1|\mathcal{Z}^j). \quad (3)$$

The grid size should be chosen sensibly with respect to measurement density such that the summation of probabilities in Eq. (2) will not exceed 1 in most cases.

The probabilities of target presence in each grid cell under detection and non-detection hypotheses at receiver $j$ are obtained using Bayes theorem as:

$$\mathrm{P}(T_i = 1|Y_i^j = 1) = \frac{\mathrm{PD}_i^j \cdot \mathrm{PT}_i}{\mathrm{PD}_i^j \cdot \mathrm{PT}_i + \mathrm{Pfa}_i^j\,(1 - \mathrm{PT}_i)}, \quad (4)$$

$$\mathrm{P}(T_i = 1|Y_i^j = 0) = \frac{(1 - \mathrm{PD}_i^j)\mathrm{PT}_i}{(1 - \mathrm{PD}_i^j)\mathrm{PT}_i + (1 - \mathrm{Pfa}_i^j)(1 - \mathrm{PT}_i)}, \quad (5)$$

where $\mathrm{PT}_i = \mathrm{P}(T_i = 1)$ represents the *a priori* probability of target in the grid cell $i$, $\mathrm{PD}_i^j = \mathrm{P}(Y_i^j = 1|T_i = 1)$ represents the probability of detection at receiver $j$ given there is a target in the grid cell $i$, and $\mathrm{Pfa}_i^j = \mathrm{P}(Y_i^j = 1|T_i = 0)$ represents the probability of false alarm at receiver $j$ in the grid cell $i$. The PD map for each source-receiver-waveform combination is precomputed using a sonar performance model which will be discussed later.

The PT map for receiver $j$ after updating the measurement data $\mathcal{Z}^j$ is obtained as:

$$\begin{aligned}\mathrm{P}(T_i = 1|\mathcal{Z}^j) =& \mathrm{P}(T_i = 1|Y_i^j = 1)\mathrm{P}(Y_i^j = 1|\mathcal{Z}^j) \\ &+ \mathrm{P}(T_i = 1|Y_i^j = 0)\mathrm{P}(Y_i^j = 0|\mathcal{Z}^j), \quad (6)\\ =& \mathrm{P}(T_i = 1|\mathcal{Z}^j)^+ + \mathrm{P}(T_i = 1|\mathcal{Z}^j)^-, \quad (7)\end{aligned}$$

where $\mathrm{P}(T_i = 1|\mathcal{Z}^j)^+$ and $\mathrm{P}(T_i = 1|\mathcal{Z}^j)^-$ represents the positive and negative PT maps for receiver $j$ respectively. The $n_R$ positive PT maps generated by $n_R$ receivers are then fused to obtain a single positive PT map after each ping; a negative PT map is obtained similarly. Some source-receiver-waveform combinations provide more confidence in their detections at certain grid cells according to their PD values given by sonar performance model predictions. We define a weighting coefficient for receiver $j$ at grid cell $i$ as:

$$w_i^j = \frac{PD_i^j}{\sum_{j=1}^{n_R} PD_i^j}. \quad (8)$$

The fused positive and negative PT maps are then obtained as the weighted average of the respective PT maps given by:

$$\mathrm{P}(T_i = 1|\check{\mathcal{Z}})^+ = \sum_{j=1}^{n_R} w_i^j \mathrm{P}(T_i = 1|\mathcal{Z}^j)^+, \quad (9)$$

$$\mathrm{P}(T_i = 1|\check{\mathcal{Z}})^- = \sum_{j=1}^{n_R} w_i^j \mathrm{P}(T_i = 1|\mathcal{Z}^j)^-. \quad (10)$$

We update the PT maps separately under the detection and non-detection hypotheses, because we further refine the positive PT map using the tracking results which will be discussed in the next subsection. We propagate the two PT maps separately and combine them after propagation to obtain the forecasted PT map.

The values of $\mathrm{PD}_i^j$ and $\mathrm{Pfa}_i^j$ are obtained from a sonar performance model for each source-receiver-waveform combination with an average omni-directional target strength in the search area [10]. Assuming the layout of the sources and receivers is fixed, the average PD maps for different source-receiver-waveform combinations can be precomputed and stored. We assume that the average false alarm rate is constant and known for each receiver; $\mathrm{Pfa}_i^j$ is computed from this given false alarm rate, the area of the search region, and the area of the grid cell. We also assume that at the beginning of the scenario each grid cell has a target probability of $p$, i.e. $P(T_i(0) = 1) = p$. After each ping, we generate a forecasted PT map for the next ping time, which becomes the *a priori* PT map for processing the next ping measurement data.

### *B. Multi-Target Tracker*

The tracker processes contacts and identifies possible targets in the presence of false alarms. This task requires the removal of a large number of false contacts, the association of true contacts, and the fusion of contact information to estimate the location and velocity of targets of interest. There is much literature on sensor data fusion and target tracking; classical references include [11] and [12]. Various types of trackers can be implemented. However an appropriate tracker implementation must consider the tradeoff between complexity and quality depending on the operation scenarios. In this work, we use a centralized, Kalman Filter (KF) tracker described in [5] for the real-time adaptive ping control application. Although the current MTT implementation uses a naive nearest neighbor data association scheme, it will serve as a baseline tracker to illustrate the procedure of incorporating the KF estimates to the PT maps. The performance of the forecaster can certainly be improved by implementing a more sophisticated data association scheme such as Multi-Hypothesis Tracking (MHT) at the cost of computational complexity [12].

We briefly describe the tracker implementation in the following. The input to the tracking algorithm is a series of contact files (scans), unique to each source-receiver-waveform and time of ping transmission, provided by the sensor network. In the current formulation, we consider only FM waveforms with a constant ping interval.

#### *Target Motion Model*

The target state vector, $X$, consists of the $x$ and $y$ components of both position and velocity, i.e. $X(t) = [x(t), y(t), \dot{x}(t), \dot{y}(t)]^T$. The discrete-time nearly constant velocity motion model is given by:

$$X_{k+1} = \Phi_k X_k + \omega_k, \quad \omega_k \sim \mathcal{N}(0, Q_k) \quad (11)$$

where $X_{k+1}$ is the target state at time $t_{k+1}$, $\Phi_k$ is the state transition matrix, and $Q_k$ is the covariance matrix representing the process noise.

*Sensor Measurement*

For detection using an FM waveform, we only have a target positional measurement $Z_k$,

$$Z_k = \begin{bmatrix} x_k \\ y_k \end{bmatrix} + \nu_k, \quad \nu_k \sim \mathcal{N}(0, R_k), \tag{12}$$

where the debiased Cartesian measurements $(x_k, y_k)$ are derived from the time-of-arrival and bearing measurements. The elements of measurement error covariance matrix $R_k$ depend on the time and bearing measurement errors [9].

*Kalman Filter Equation*

The target state estimate and its covariance matrix at time $t_k$ is denoted by $X(k|k)$ and $P(k|k)$, respectively. Given the initial target state estimate and error covariance matrix, the recursive Kalman Filter equations are described as follows:

$$X(k|k-1) = \Phi_{k-1} X(k-1|k-1) \tag{13}$$

$$P(k|k-1) = \Phi_{k-1} P(k-1|k-1) \Phi_{k-1}^T + Q_{k-1} \tag{14}$$

$$L(k) = P(k|k-1) C^T \left( C P(k|k-1) C^T + R_{k-1} \right)^{-1} \tag{15}$$

$$X(k|k) = X(k|k-1) + L(k) \tilde{y}(k) \tag{16}$$

$$P(k|k) = (I - L(k)C)\, P(k|k-1), \tag{17}$$

where $\tilde{y}(k) = [x_k, y_k]^T - CX(k|k-1)$, $I$ is the $4 \times 4$ identity matrix and

$$C = \begin{bmatrix} 1 & 0 & 0 & 0 \\ 0 & 1 & 0 & 0 \end{bmatrix}.$$

As for the initial target state estimate, we use the first converted measurement with zero initial velocity estimate.

*Tracker Logic*

The tracking algorithm recursively processes the sets of contacts from the sequence of pings initiated at times $(t_1 \leq t_2 \leq \cdots)$. The first ping at time $t_1$ contains the set of contacts $\{Z_q^j(1), q = 1, \cdots, n_j, j = 1, \cdots, n_R\}$. Each of these is used to initiate a *tentative* track with a state estimate and its covariance matrix. At each subsequent ping time $t_k$, we have a set of tracks (some of which are *confirmed*) from the previous processing step at time $t_{k-1}$, and a current set of contacts $\{Z_q^j(k), q = 1, \cdots, n_j, j = 1, \cdots, n_R\}$. Each track is predicted forward from time $t_{k-1}$ to the current time $t_k$. Then the nearest neighbor contact for each track is selected among all *validated* contacts. Validated contacts are those that satisfy the following threshold condition, for a given $\chi^2$ parameter

$$\tilde{y}(k)^T S(k)^{-1} \tilde{y}(k) \quad < \chi^2, \tag{18}$$

where the innovation covariance matrix, $S(k)$, is equal to $CP(k|k-1)C^T + R_{k-1}$, and the nearest neighbor is that contact for which the LHS of the above equation is smallest. If no validated contact exists, no track update is performed. We continue in this manner for all tracks, and remaining contacts are used to initiate new tracks. A track is confirmed when it associates $M$ contacts within $N$ scans of data. Also, once a track is confirmed, it is terminated after $K$ consecutive missed detections.

### C. Tracking Scoring

The output of the tracking algorithm contains multiple tracks (tentative tracks and confirmed tracks). To obtain the PT map, one must map the state estimates and their covariance matrices to the probability of target presence on the grid $G$. Since not all the tracks are originated from true targets, we compute a track score to describe how likely (or unlikely) it is that the reconstructed track originates from detections of the true target by considering kinematic and signal-related contributions.

The track score is defined as the log of the likelihood ratio (LLR) of the hypothesis that the set of observations in the track are from the same target and the hypothesis that the track is a collection of false alarms. The initial track score is estimated from the *a priori* PT map and the grid cell Pfa. Thereafter, upon the receipt of data on scan $m$, the score for track $n$ is updated according to the relationship [12]:

$$L_n(m) = L_n(m-1) + \Delta L(m), \tag{19}$$

where

$$\Delta L(m) = \begin{cases} \ln(1 - \text{PD}) & \text{no track update on scan } m \\ \Delta L_U & \text{track update on scan } m \end{cases}$$

$$\Delta L_U = \ln \left\{ \frac{\text{PD} \cdot V_C}{2\pi \text{Pfa} \sqrt{|S|}} \right\} - \frac{d^2}{2}$$

$\text{PD} =$ estimated probability of detection

$\text{Pfa} =$ estimated probability of false alarm

$V_C =$ volume of the measurement validation region

$S =$ innovation covariance matrix

$d^2 =$ normalized statistical distance function

The track score for track $n$ is updated recursively using Eq. (19) for all the scans at each ping time. The updated LLR score can then be directly converted to the probability of a track $X_j$, being a true target through [12]:

$$\text{P}(X_j) = \frac{\exp(L_j)}{1 + \exp(L_j)}. \tag{20}$$

Let $X^A$ denote the set of active tracks (tracks that are updated using at least one contact) at the current ping time and $N^A$ the cardinality of the set $X^A$. To convert the active track estimates to the probability on the grid cell, we compute the weighting coefficients for those tracks in $X^A$. When there is no contact updating a track at the current ping time (although the track is being propagated using KF propagation equation), that track does not need to be considered at the current ping time because that track information is not momentarily included in evaluation of the positive PT map, but rather in the negative PT map. Therefore, the track scores for those tracks not included in the set $X^A$ are not included in the computation of the

weighting coefficients or the mapping to the positive PT map. The weighting coefficient for the active track is computed as:

$$\tilde{w}_n = \frac{\mathrm{P}(X_n)}{\sum_{j=1}^{N^A} \mathrm{P}(X_j)}, \quad X_n \in X^A. \tag{21}$$

### D. Propagation

A second positive PT map is generated using the KF tracker output. This new positive PT map and the negative PT map from the Bayes update are propagated separately: the positive map using the KF tracker forecasted estimates and the negative map using a diffusion process model. We assume that the forecasting frequency is high relative to the target speed and that there is no new target at the next forecast time.

*Positive PT Map*

The KF propagation equations (13) and (14) are used to produce forecasted estimates of the active tracks at the next ping time. We then compute the probability of target presence on each grid cell for each active track using the state estimate and its covariance matrix. Assuming that targets are independent and the probability that there is more than one target in a grid cell is small, the probability on each grid cell accounting for all active tracks is approximated as a weighted sum of the individual probabilities with weights corresponding to their track scores. The resulting probability map is then normalized to the first positive PT map that was generated using Eq. (9), such that the sums of all grid cell probabilities of each map are equal. The first positive PT map is then discarded. We describe the PT map conversion in the following.

The probability of target presence on each grid cell accounting for all active tracks is given by a weighted sum of the probability contributed by each individual track as:

$$\begin{aligned}&\mathrm{P}(T_i(k+1)=1|\check{X}(k+1|k),\check{P}(k+1|k))\\&=\sum_{j=1}^{N_A}\tilde{w}_j\int_{(x,y)\in g_i}\mathcal{N}(CX_j(k+1|k),CP_j(k+1|k)C^T)dxdy,\end{aligned} \tag{22}$$

where $(X_j(k+1|k), P_j(k+1|k))$ denotes the state estimate and covariance matrix of active track $j$, $\check{X}(k+1|k) = \{X_1(k+1|k), \cdots, X_{N^A}(k+1|k)\}$ and $\check{P}(k+1|k) = \{P_1(k+1|k), \cdots, P_{N^A}(k+1|k)\}$. The probability is then renormalized to match the sum of the probability of the positive PT map after the Bayes update to obtain the forecasted positive PT map as:

$$\mathrm{P}(T_i(k+1)=1)^+ = \eta\cdot\mathrm{P}(T_i(k+1)=1|\check{X}(k+1|k),\check{P}(k+1|k)), \tag{23}$$

$$\eta = \frac{\sum_{i=1}^{N_g}\mathrm{Pr}(T_i(k)=1|\check{\mathcal{Z}}(k))^+}{\sum_{i=1}^{N_g}\mathrm{P}(T_i(k+1)=1|\check{X}(k+1|k),\check{P}(k+1|k))}. \tag{24}$$

*Negative PT Map*

The negative PT map is propagated using a Brownian motion diffusion model as described in [13]. The target motion in the $x$ and $y$ directions are defined by a normally distributed random variable $\mathcal{N}(0, \sigma^2 t)$. The Fokker-Planck (FP) equation for the Brownian motion is given by:

$$\frac{\partial\rho}{\partial t} = \frac{1}{2}\sigma^2\frac{\partial^2\rho}{\partial x^2} + \frac{1}{2}\sigma^2\frac{\partial^2\rho}{\partial y^2}, \tag{25}$$

where $\rho(x, y, t)$ represents the probability density of target presence at time $t$ in the negative PT map. The FP equation is solved using finite-difference methods by discretizing the variables $x, y$, and $t$ as:

$$x = m\delta, \quad m = 1, 2, \cdots, n_x \tag{26}$$

$$y = n\delta, \quad n = 1, 2, \cdots, n_y \tag{27}$$

$$t = k\Delta t, \quad k = 1, 2, \cdots, n_t, \tag{28}$$

where $\delta$ is the width of each grid cell on $G$. The number of discretized cells in each direction is defined by $n_x$ and $n_y$. The discrete-time increment is defined by $\Delta t$ and the number of forecast times by $n_t$. The above finite-difference equations are applied to Eq. (25) resulting in:

$$\begin{aligned}\rho_{m,n,k+1} = \rho_{m,n,k} + \Delta t\Bigg(&\frac{\sigma^2}{2\delta x^2}\left(\rho_{m-1,n,k} - 2\rho_{m,n,k} + \right.\\&\left.\rho_{m+1,n,k}\right) + \frac{\sigma^2}{2\delta y^2}\left(\rho_{m,n-1,k} - 2\rho_{m,n,k} + \rho_{m,n+1,k}\right)\Bigg).\end{aligned} \tag{29}$$

Given the *a priori* negative PT map, the above equation updates the forecasted probability of target presence under the non-detection hypothesis as:

$$\mathrm{P}(T_i(k+1)=1)^- = \rho_{m,n,k+1}, \quad i \leftrightarrow (m, n). \tag{30}$$

The forecasted PT map is obtained as a summation of the forecasted positive PT map and the forecasted negative PT map given in Eqs. (23) and (30) as:

$$\begin{aligned}&\mathrm{P}(T_i(k+1)=1) = \mathrm{P}(T_i(k+1)=1)^+ + \mathrm{P}(T_i(k+1)=1)^-,\\&\quad i = 1, 2, \cdots, N_g.\end{aligned} \tag{31}$$

## III. Simulation

The probability of target forecaster is run at the end of each ping to generate the PT map at the next ping time. In this section, we illustrate that the PT maps provide accurate multistatic operational pictures. They include the probability generated by target-originated contacts as well as by false contacts for further investigation in subsequent pings. The PT maps also include the probability of targets that might be missed and the probability that no target is present.

In this example, there are 3 sources and 4 receivers deployed in the search area of 40 km $\times$ 40 km. There are two targets: target 1 (T1) is heading southeast with a constant speed of 6 knots and target 2 (T2) is heading east with a constant speed of 5 knots. The scenario is illustrated in Figure 1. We use a contact simulator to generate true and false contacts. The contact simulator integrates a range-dependent sonar performance model, an aspect-dependent target strength model, measurement errors and false contact distributions in number,

time-of-arrival, bearing and SNR. The simulator outputs true and false contacts. A description of the implementation of the contact simulator is given in [10].

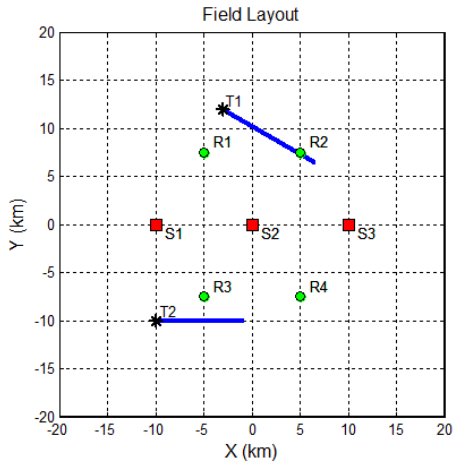


Figure 1. Simulated scenario: three sources (red square), four receivers (green circle) and two targets (blue line). Asterisks indicate the start of the tracks.

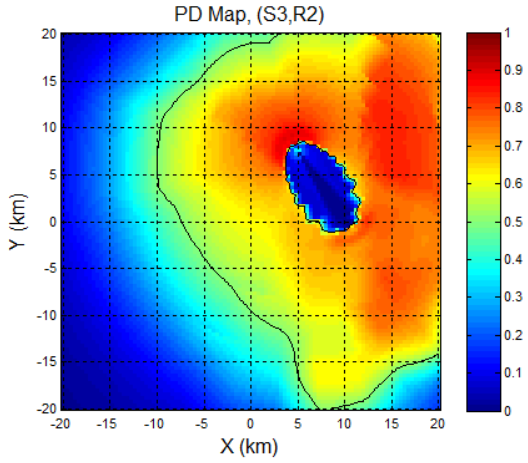


Figure 2. The PD map for source 3, receiver 2 and FM waveform combination generated with a omni-directional target strength of 4 dB and a target doppler of 3 knots.

We discretize the search area into $N_g = 100 \times 100$ grid cells. We begin the scenario with $\mathrm{P}(T_i(0) = 1) = 10^{-4}$ for $i = 1, 2, \cdots, N_g$. The Pfa of each grid cell is set to 0.0012, which corresponds to an average false alarm rate of 12 per ping interval in the search area. In this example, a ping is generated every 60 seconds using an FM waveform and a round-robin policy among sources. The PD maps are precomputed for each source and receiver pair using the sonar performance model. We assume an average omni-directional target strength of 4 dB, a target doppler of 3 knots and a signal fluctuation of 10 dB to generate the PD maps. A PD map for source 3, receiver 2 and FM waveform combination is shown in Figure 2. The track initiation parameters $(M/N)$ are not critical for this example since the forecaster considers both tentative and unconfirmed tracks. We set the track initiation parameter $(M/N)$ to $(1/1)$ and the kill parameter $K$ to 8.

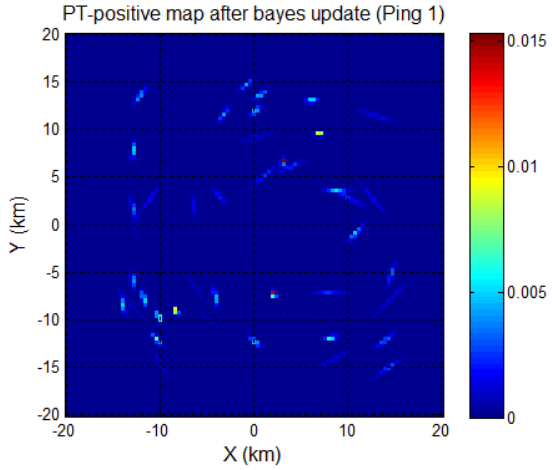


Figure 3. The positive PT map after Bayes update for ping 1.

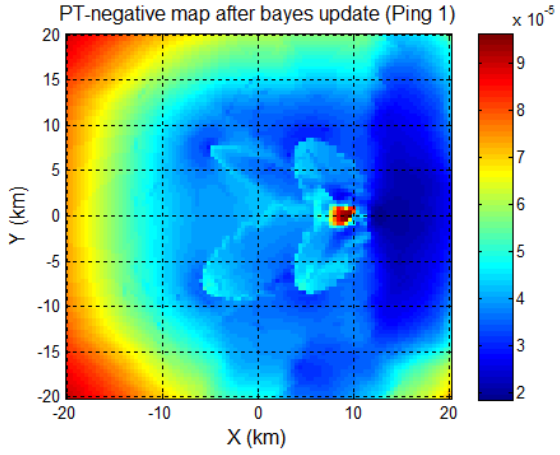


Figure 4. The negative PT map after Bayes update for ping 1.

The positive and negative PT maps after Bayes update for ping 1 (source 3) are shown in Figures 3 and 4, respectively. The PT values under the detection hypothesis increase in the grid cells which contain contacts (Figure 3). The PT values under the non-detection hypothesis decrease from the *a priori* PT corresponding to the weighted average PD values of the grid cells (Figure 4).

Since many of the contacts are false alarms, instead of directly propagating the positive PT map using a diffusion process model, the contacts are further processed by the KF

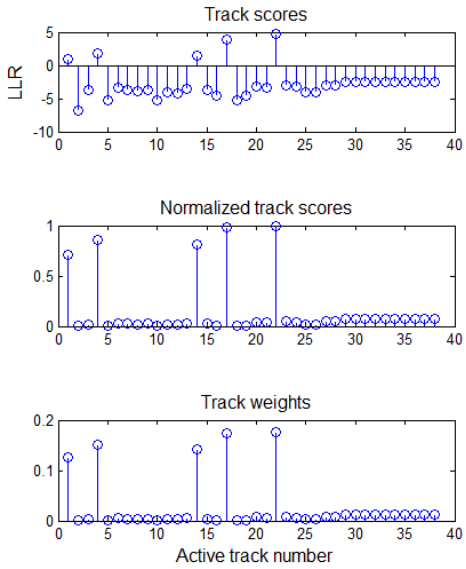


Figure 5. Track scores and track weights for all active tracks after ping 1.

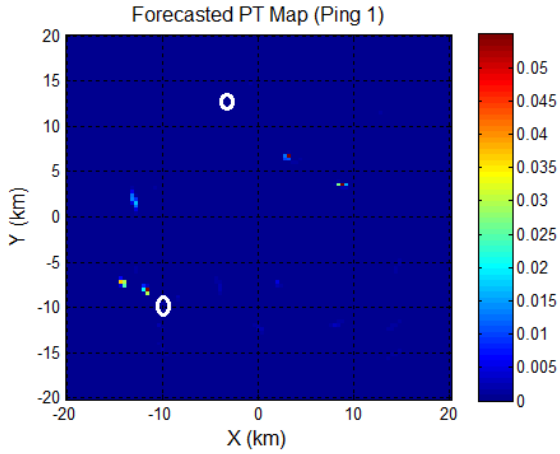


Figure 6. Forecasted PT map at ping time 2. White circles indicate the locations of true targets.

tracker to obtain a more accurate representation of the positive PT map. Figure 5 shows the number of active tracks generated after ping 1 and their LLR scores. In this simulation, ping 1 generates a total of 43 contacts at the receivers, and there are 5 tracks with positive LLR scores. Initially, none of the tracks with positive LLR scores corresponds to a true target track. The negative PT map is propagated using a Brownian motion model with a diffusion rate of 5 knots. The forecasted PT map at ping time 2 is obtained by combining the positive and

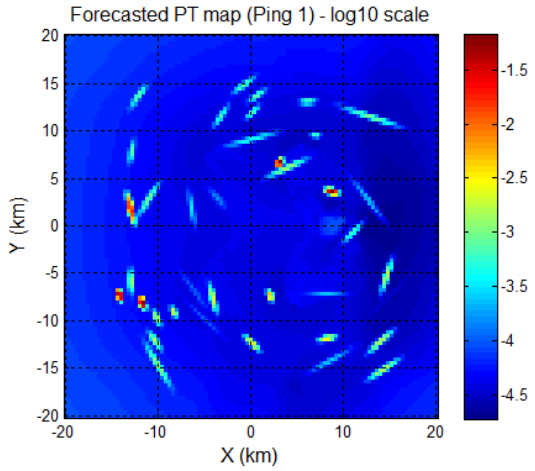


Figure 7. Forecasted PT map at ping time 2 in Log10 scale.

negative PT maps and is shown in Figure 6. The logarithmic scale graph for the forecasted PT map at ping time 2 is shown in Figure 7 for better visualization. After ping 1, PT values in the far east side decrease corresponding to the higher PD values of the grid cells in the far east side. The peak PT values are distributed throughout the search area corresponding to the contact locations with varying PT values according to the normalized track scores. Search effort must be expended to continue the true/false investigation of tracks in addition to continually checking the grid cells that might be overlooked due to non-detection. The forecasted PT map accounts for all these probabilities in a single operational picture.

The number of active tracks and their track scores after ping 4 are displayed in Figure 8. After processing 16 scans of contact detections, the two active tracks which correspond to the true target tracks can clearly be seen. The forecasted PT maps at ping time 5 in linear and logarithmic scale are shown in Figures 9 and 10. The true target tracks correspond to the highest PT values in the forecasted PT map. The peaks corresponding to the false tracks are also seen in the PT map. The current track weighting scheme uses an exponential scale, and therefore all the tracks with positive LLR are considered as high-probability true tracks and are weighed nearly equally. The probability of those tracks are continued to be tracked under the non-detection hypothesis even when they are not associated with any contact in the current ping (better seen in Figure 10). We can also see that the probabilities in the dark blue area of Figure 10 decrease two order of magnitude after 4 pings. This means that the search effort should now be expended more at the peaks and the edges. Different weighting schemes will affect how much emphasis the search effort places on the active tracks. The tracker results can further be improved with a better data association scheme such as MHT [12]. Other classification features can also be included for improved true/false discrimination. All of these aspects will be addressed in future work.

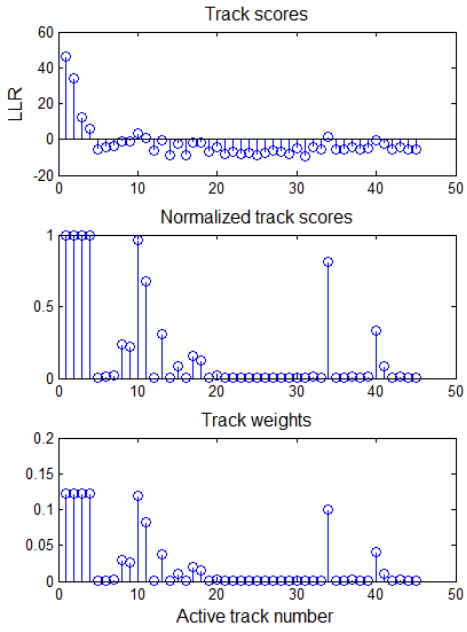


Figure 8. Track scores and track weights for all active tracks after ping 4.

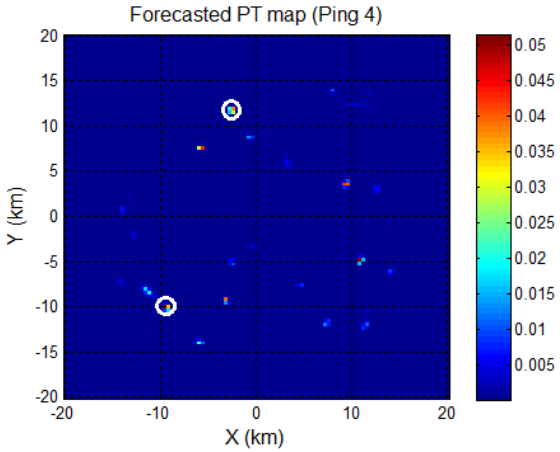


Figure 9. Forecasted PT map at ping time 5. White circles indicate the locations of true targets.

## IV. Conclusions

We have presented a probability of target presence forecaster. We have illustrated that the PT maps represent accurate operational pictures by considering both detection and tracking results. The forecasted PT map includes not only the probabilities of true/false tracks with emphasis on true tracks according to their LLR track scores but also the missed target probabilities. The forecasted PT map can be used in conjunction with the PD maps from a sonar performance model in ping control solutions for search missions. Future work will investigate using the forecasted PT map as a metric for ping control optimization. We will also extend the formulation to include doppler information and explore different track weighting and classification schemes for improved true/false discrimination.

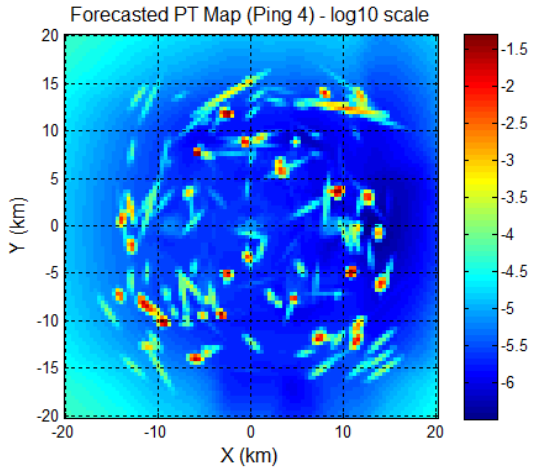


Figure 10. Forecasted PT map at ping time 5 in Log10 scale.

## References


[1] D. Grimmett, and S. Coraluppi, "Multistatic Active Sonar System Interoperability, Data Fusion, and Measures of Performance," *NURC Technical Report NURC-FR-2006-004*, Apr. 2006.

[2] B. I. Incze, and S. Simakov,"Anti-Submarine Warfare Residual Risk and its Computation," *TTCP Technical Report TR-MAR-9-2011*, Nov. 2010.

[3] D. W. Krout, M. A. El-Sharkawi, W. L. J. Fox, and M. U. Hazen, "Intelligent Ping Sequencing for Multistatic Sonar Systems," *Proc. of the 9th Intl. Conf. on Information Fusion*, Florence, Italy, Jul. 2006.

[4] A. Saksena, and I-J. Wang, "Dynamic Ping Optimization for Surveillance in Multistatic Sonar Buoy Networks with Energy Constraints," *Proc. of the 47th IEEE Conf. on Decision and Control*, Cancun, Mexico, Dec. 2008.

[5] S. Coraluppi, and D. Grimmett, "Multistatic Sonar Tracking," *Proc. of the SPIE Conf. on Signal Processing, Sensor Fusion, and Target Recognition XII*, Orlando, Florida, Apr. 2003.

[6] O. Erdinc, P. Willett, and Y. Bar-Shalom, "Probability Hypothesis Density Filter for Multitarget Multisensor Tracking," *Proc. of the 8th Intl. Conf. on Information Fusion*, Philadelphia, PA, Jul. 2005.

[7] B. Vo, and W. Ma, "The Gaussian Mixture Probability Hypothesis Density Filter," *IEEE Trans. on Signal Processing*, vo. 54, no. 11, pp. 4091-4104, Nov. 2006.

[8] R. Mahler, "Multi-target Bayes filtering via first-order multi-target Moments," *IEEE Trans. Aerospace and Electronic Systems*, vol. 39, no. 4, pp.1152-1178, 2003.

[9] S. Coraluppi, "Multistatic Sonar Localization," *IEEE Journal of Oceanic Engineering*, vol. 31, no. 4, pp. 964-974, Oct. 2006.

[10] D. Grimmett, C. Wakayama, and R. Ricks, "Simulation of Passive and Multistatic Active Sonar Contacts," *4th Intl. Conf. on Underwater Acoustic Measurements: Technologies & Results*, Kos Island, Greece, Jun. 2011.

[11] Y. Bar-Shalom, and X. R. Li, *Multitarget-Multisensor Tracking: Principles and Techniques*, YBS Publishing, 1995.

[12] S. Blackman, and R. Popoli, *Design and Analysis of Modern Tracking Systems*, Artech House, Norwood, MA, 1999.

[13] D. W. Krout, W. L. J. Fox, and M. A. El-Sharkawi, "Probability of Target Presence for Multistatic Sonar Ping Sequencing," *Journal of Oceanic Engineering*, vol. 34, no. 4, pp. 603-609, Oct. 2009.